2021 IEEE Intelligent Vehicles Symposium (IV)
July 11-17, 2021. Nagoya, Japan

Opportunistic Strategy for Cooperative Maneuvering Using Conflict Analysis

Hao M. Wang, Sergei S. Avedisov, Ahmed H. Sakr, Onur Altintas, and Gábor Orosz

***Abstract*— In this paper, we propose an optimization-based strategy that utilizes vehicle-to-everything (V2X) communication in order to resolve conflicts between vehicles of different automation levels. The strategy consists of a decision checking mechanism and a control law to adjust the decision of an ego vehicle in a certain maneuver based on status update messages received from a remote vehicle involved in that maneuver. Using numerical simulations with real highway data, we demonstrate the proposed opportunistic strategy and show how it improves safety and maximizes the time efficiency of the ego vehicle. We also highlight the benefits of the strategy by comparing the results with an existing conservative strategy.**

I. Introduction

Maneuvers of road participants may involve conflicts if their trajectories cross with each other such that they appear in the same location at the same time. Examples include merges, roundabouts, unprotected left turns, intersections and other scenarios. Mismanaging such conflicts may compromise safety and cause accidents. In traffic scenarios where all vehicles are highly automated, prior results demonstrated the benefits of vehicle-to-everything (V2X) communication technologies in improving safety and performance by enabling vehicles to seek agreements about their future maneuvers [1]–[3]. In these scenarios one may use a variety of methods to design decision making, motion planning, and control algorithms [4]–[6]. However, for the next few decades, it is reasonable to assume a mixed traffic environment with vehicles of different automation and cooperation levels (including human-driven vehicles) [7]–[9]. This demands a systematic way of resolving conflicts in such mixed environments.

Earlier work [10], [11] looked at the so-called capture set in state space (where conflicts are unavoidable) while considering both cooperative and competitive behaviors between vehicles. In our recent work [12], we proposed a tool called conflict analysis to handle cooperative maneuvering between road participants with different automation levels. Utilizing formal logic, we calculated the so-called no-conflict, conflict, and uncertain domains in the state space. The corresponding conflict charts enable fast and reliable decision making and controller design. In this paper, we extend the conflict analysis by introducing an optimization-based opportunistic strategy which can improve performance while guaranteeing a conflict-free maneuver at the same time.

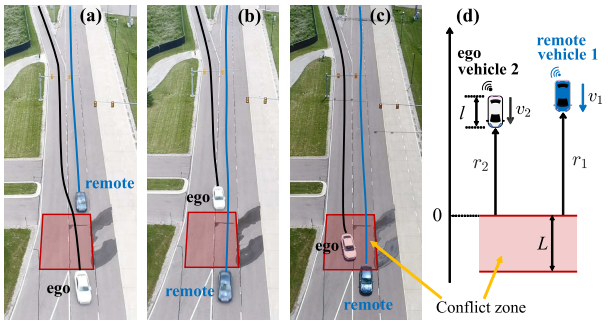

Fig. 1. Cooperative maneuvering with potential conflict. (a) the ego vehicle merges ahead without conflict, (b) the ego vehicle merges behind without conflict, and (c) a conflict occurs; (d) the generalized model of cooperative maneuvering, where the red-shaded region is the conflict zone.

Fig. 1(a)-(c) show three realizations of a maneuver, where the ego vehicle (white) merges ahead of, merges behind, and has a conflict with the remote vehicle (blue), respectively. Here we define a conflict zone of a finite size, representing a safety buffer between vehicles where the shape and size may vary based on road configurations and type of maneuver. In the merge maneuver, we consider this zone to be of a rectangular shape and fixed to the ground around the end of the ramp; see the red shaded area in Fig. 1. To prevent conflict, the two vehicles must not be present inside the conflict zone at the same time. We resolve conflicts from the perspective of the ego vehicle because it must yield to vehicles traveling on the main road based on traffic rules. We assume that the ego vehicle receives status sharing messages via V2X from the remote vehicle that contain the current position and speed of the remote vehicle. One example of a standardized status sharing message is the basic safety message (BSM) [13]. In conflict analysis, we interpret messages transmitted by remote vehicles by means of conflict charts, which allow us to devise conflict-free controllers for the ego vehicle based on the message content and the state of the ego vehicle. By solving a constrained optimization problem, we derive an opportunistic strategy that maximizes the possibility of the ego vehicle to merge ahead while satisfying the conflict-free condition. This reduces the conservatism in the strategy proposed in [12] (referred to as conservative strategy) in terms of the time efficiency of ego vehicle. These benefits are demonstrated by using traffic data taken on a highway in south-east Michigan.

Hao M. Wang and Gábor Orosz are with the Department of Mechanical Engineering, University of Michigan, Ann Arbor, MI 48109, USA. {haowangm, orosz}@umich.edu.

Sergei S. Avedisov and Onur Altintas are with Toyota Motor North America R&D – InfoTech Labs, Mountain View, CA 94043, USA. {sergei.avedisov, onur.altintas}@toyota.com.

Ahmed H. Sakr is currently with the Department of Electrical and Computer Engineering, University of Windsor, Windsor, ON, N9B 3P4, Canada. ahmed.sakr@uwindsor.ca. He was with Toyota Motor North America R&D – InfoTech Labs, Mountain View, CA 94043, USA during the time when the results were generated.

Gábor Orosz is also with the Department of Civil and Environmental Engineering, University of Michigan, Ann Arbor, MI 48109, USA.

2021 IEEE Intelligent Vehicles Symposium (IV) | 978-1-7281-5394-0/21/$31.00 ©2021 IEEE | DOI: 10.1109/IV48863.2021.9575586

II. Modeling Vehicle Dynamics

Consider the scenario depicted in Fig. 1(a)-(c) where the ego vehicle (white) is joining the main carriageway while the remote vehicle (blue) is approaching along the main road. The conflict zone is located towards the end of the ramp as indicated by the red rectangle. In this paper, we ignore the lateral dynamics of both vehicles and consider the model shown in Fig. 1(d). Hereafter, the remote and ego vehicles are referred to as vehicles 1 and 2, respectively. Here r_1 and r_2 denote the distances of the vehicles from the conflict zone, and v_1 and v_2 denote their longitudinal velocities. The length of the conflict zone is denoted by L, the length of both vehicles is l, and we define $s := L + l$.

By neglecting the air and rolling resistances, the longitudinal dynamics of the vehicles can be given by

$$\begin{aligned} \dot{r}_1 &= -v_1, & \dot{v}_1 &= \mathrm{sat}(u_1), \\ \dot{r}_2 &= -v_2, & \dot{v}_2 &= \mathrm{sat}(u_2), \end{aligned} \tag{1}$$

where the dot represents the derivative with respect to time t and the negative signs appear since the vehicles are traveling towards the negative direction. Moreover, u_1 and u_2 are the control inputs, which are limited by the acceleration limits given by the saturation function

$$\mathrm{sat}(u) = \begin{cases} a_{\min}, & \text{if } u \in (-\infty, a_{\min}], \\ u, & \text{if } u \in (a_{\min}, a_{\max}), \\ a_{\max}, & \text{if } u \in [a_{\max}, \infty), \end{cases} \tag{2}$$

when $v \in (v_{\min}, v_{\max})$. For $v = v_{\min}$, we replace $a_{\min}$ with 0, since the vehicle is not allowed to decelerate; for $v = v_{\max}$, we replace $a_{\max}$ with 0, since the vehicle is not allowed to accelerate. Table I summarizes all parameter values used that correspond to typical highway driving. We assume that these limits are known to the ego vehicle. Notice that $a_{\max,2}$ and $a_{\min,2}$ are not necessarily the physical limits of the ego vehicle, but are parameters that can be chosen by the users. Also, $v_{\min,2}$ is set to zero, meaning the ego vehicle is allowed to stop along the ramp if necessary. We define the state of the system (1) as $x := [r_1, v_1, r_2, v_2]^\top \in \Omega$, where $\Omega := [-s, \infty) \times [v_{\min,1}, v_{\max,1}] \times [-s, \infty) \times [v_{\min,2}, v_{\max,2}]$.

As mentioned before, when designing the decision making and control algorithms for the ego vehicle, the status sharing messages which contain the current status of the remote vehicle (r_1 and v_1) are used. We define the initial time to be the time when the first status sharing packet is received by the ego vehicle. Note that while the remote vehicle shares its motion information via V2X communication, we do not have control over its motion. We can only assign the input u_2 and have no knowledge about the exact value of u_1 (except for its limits). Under these conditions, our goal is to design decision making and control algorithms for the ego vehicle that ensure time-efficient and conflict-free maneuvers.

TABLE I

Parameters values used in the paper.

L	20 [m]	l	5 [m]
$a_{\min,1}$	-4 [m/s^2]	$a_{\min,2}$	-4 [m/s^2]
$a_{\max,1}$	2 [m/s^2]	$a_{\max,2}$	2 [m/s^2]
$v_{\min,1}$	20 [m/s]	$v_{\min,2}$	0 [m/s]
$v_{\max,1}$	35 [m/s]	$v_{\max,2}$	35 [m/s]

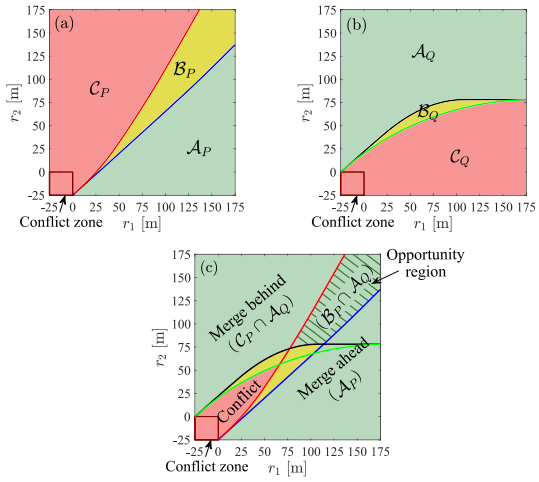

Fig. 2. Conflict charts in the (r_1, r_2)-plane for $v_1 = 28$ [m/s] and $v_2 = 25$ [m/s]. (a)-(c) Conflict charts for merge ahead, merge behind, and the unified conflict chart. The opportunity region in panel (c) is highlighted by stripes.

III. Conflict Analysis

In this section, we review the conflict analysis proposed in [12], which provides a formal logic based tool for decision making and control design for conflict prevention. Moreover, we point out the conservatism of the decision making rule in [12] and highlight the potential benefits that may be obtained by the opportunistic strategy discussed further below.

A. Conflict Charts

A conflict is defined by both vehicles being in the conflict zone at the same time. This can be formally expressed by the proposition

$$C := \{\exists t, r_1(t) \in [-s, 0] \wedge r_2(t) \in [-s, 0]\}, \tag{3}$$

and thus a conflict-free maneuver is given by

$$\neg C = \{\forall t, r_1(t) \notin [-s, 0] \vee r_2(t) \notin [-s, 0]\}, \tag{4}$$

where symbols $\wedge$ (and), $\vee$ (or), and $\neg$ (negation) are used. Moreover, $\neg C$ can be decoupled into the following two cases:

$$\begin{aligned} P &:= \{\exists t, r_1(t) = 0 \wedge r_2(t) < -s\}, \\ Q &:= \{\exists t, r_1(t) = -s \wedge r_2(t) > 0\}, \end{aligned} \tag{5}$$

where the proposition P implies that the ego vehicle merges ahead of remote vehicle without a conflict (see Fig. 1(a)), while proposition Q implies that the ego vehicle merges behind the remote vehicle without a conflict (see Fig. 1(b)). One can show that

$$P \vee Q \iff \neg C. \tag{6}$$

That is, to ensure a non-conflicting merge we need to show that either a conflict-free merge ahead or a conflict-free merge behind exists. This concept can be generalized to multiple-vehicle cases by considering pairwise conflicts and

can be extended to many other traffic scenarios involving potential conflicts; unprotected left-turns, lane changes, etc.

One can further decompose proposition P (vehicle 2 merging ahead) into three cases:

(i) No-conflict case: vehicle 2 is able to merge ahead without conflict independent of the motion of vehicle 1.
(ii) Uncertain case: vehicle 2 may be able to merge ahead without conflict depending on the motion of vehicle 1.
(iii) Conflict case: vehicle 2 is not able to merge ahead without conflict independent of the motion of vehicle 1.

Cases (i), (ii) and (iii) correspond to three disjoint sets in the state space of the system (1), defined by

$$\mathcal{A}_P := \{x \in \Omega | \forall u_1(t), \exists u_2(t), P\}, \tag{7}$$

$$\mathcal{B}_P := \{x \in \Omega | (\exists u_1(t), \forall u_2(t), \neg P) \wedge (\exists u_1(t), \exists u_2(t), P)\}, \tag{8}$$

$$\mathcal{C}_P := \{x \in \Omega | \forall u_1(t), \forall u_2(t), \neg P\}. \tag{9}$$

Fig. 2(a) shows these sets on the (r_1, r_2)-plane for velocities $v_1 = 28$ [m/s] and $v_2 = 25$ [m/s], where $\mathcal{A}_P$, $\mathcal{B}_P$ and $\mathcal{C}_P$ are shaded as green, yellow and red, respectively; see [12] for detailed derivations. By locating the current vehicle state x on this chart, one can reason about conflict in terms of merge ahead. This chart is referred to as a conflict chart. Similarly, proposition Q can be decomposed into no-conflict, uncertain and conflict cases using merge behind instead of merge ahead. The corresponding sets in state space are denoted by $\mathcal{A}_Q$, $\mathcal{B}_Q$, and $\mathcal{C}_Q$, respectively. They are visualized with green, yellow and red shadings in Fig. 2(b), respectively.

The conflict charts for merging ahead and behind cases can be combined to derive the unified conflict chart shown in Fig. 2(c). We color the unified conflict chart using the following rule: superimposing a green region with any other region gives green; superimposing a yellow region with a yellow or red region gives yellow; and superimposing two red regions gives red. That is, the green region in the unified conflict chart is where a conflict can be prevented by the ego vehicle (either by merging ahead or by merging behind the remote vehicle), while in the red region conflict is unavoidable. In the yellow region conflict may or may not be prevented depending on the motion of the remote vehicle. Notice that the boundaries separating these regions stretch far into the state space, enabling an early decision making when the vehicles are far away from the conflict zone.

B. Conservative Strategy and Potential Opportunity

In [12], the following conservative decision making rule was proposed in the green region of the unified conflict chart:

$$\text{decision} = \begin{cases} \text{merge ahead}, & \text{if } x(0) \in \mathcal{A}_P, \\ \text{merge behind}, & \text{if } x(0) \notin \mathcal{A}_P,\ x(0) \in \mathcal{A}_Q. \end{cases} \tag{10}$$

Within $\mathcal{A}_P$ (green region below the blue boundary in Fig. 2(c)), there is no conflict with respect to proposition P and vehicle 2 is able to merge ahead without a conflict independent of the motion of vehicle 1. The decision for this region is indeed merge ahead. Note that merging ahead leads to higher time efficiency and thus has priority over merging behind. When merging ahead without conflict is not guaranteed but merging behind without conflict is guaranteed independent of the motion of vehicle 1 (green region above the blue boundary in Fig. 2(c)), then vehicle 2 decides to merge behind. Once the decision is made at the initial time, vehicle 2 sticks to it and executes it by choosing an appropriate control law. In [12], two separate controllers were designed for merging ahead and behind, which ensured conflict-free merge by keeping the evolution of the state inside the no-conflict sets $\mathcal{A}_P$ and $\mathcal{A}_Q$, respectively. We refer to the above decision making rule and the corresponding control laws as the conservative strategy in the rest of the paper.

To understand the conservatism one may notice that the merge behind decision is applied in two different regions of the state space. In $\mathcal{C}_P \cap \mathcal{A}_Q$ (green region above the red boundary in Fig. 2(c)), merging ahead without conflict is not possible, and thus, merge behind is the only choice. On the other hand, in $\mathcal{B}_P \cap \mathcal{A}_Q$ (striped region between the red and blue boundaries in Fig. 2(c)), merging ahead without a conflict may be possible depending on the future behavior of vehicle 1. This may offer potential opportunities for vehicle 2 to merge ahead. The conservative strategy makes the decision of merge behind without pursuing the opportunity to merge ahead actively. We name this striped region in conflict chart the opportunity region, and in the next section we propose an opportunistic strategy, which tries to merge ahead in this region, while still ensuring a conflict-free merge.

IV. Opportunistic Strategy

In this section, we focus on the opportunity region $\mathcal{B}_P \cap \mathcal{A}_Q$ revealed by the conflict analysis (striped region in Fig.2(c)). We propose an opportunistic strategy which consists of a decision checking mechanism and an optimization-based controller.

A. Decision Checking Mechanism

As conflict analysis shows, if the initial state is in the opportunity region (i.e., $x(0) \in \mathcal{B}_P \cap \mathcal{A}_Q$), then the ego vehicle may be able to merge ahead without a conflict depending on the motion of the remote vehicle. To prevent conflict, the ego vehicle decides to pursue the opportunity to merge ahead, while ensuring that a conflict-free merge behind is still guaranteed in the case that merge ahead is not possible. To execute this decision, one needs to solve a constrained optimization problem, which is discussed in detail in the next subsection. This initial decision will be revised and settled down to either merge ahead or behind later on as updates about the status of the remote vehicle become available. The decision can be changed to merge ahead if the system state evolves into the no-conflict set with respect to merge ahead ($\mathcal{A}_P$), i.e., the trajectory crosses the blue boundary in conflict charts (see Fig. 2(c)). On the other hand, the decision must be finalized as merge behind if the trajectory crosses the red boundary and enters $\mathcal{C}_P \cap \mathcal{A}_Q$ region.

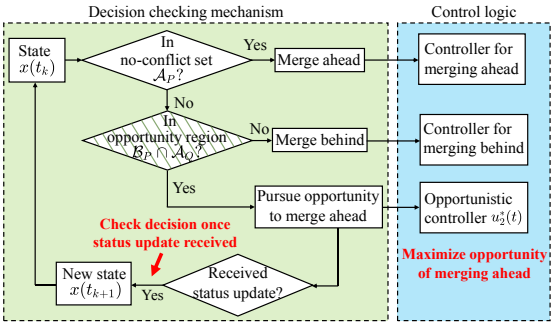

Fig. 3. Block diagram of the opportunistic strategy.

This decision making rule is summarized as

$$\text{decision} = \begin{cases} \text{stick to merge ahead,} & \text{if } x(t_k) \in \mathcal{A}_P, \\ \text{pursue opportunity to merge ahead,} & \text{if } x(t_k) \in \mathcal{B}_P \cap \mathcal{A}_Q, \\ \text{stick to merge behind,} & \text{if } x(t_k) \in \mathcal{C}_P \cap \mathcal{A}_Q, \end{cases} \tag{11}$$

where $t_k, k = 0, 1, \ldots$ represent the time when status sharing packets are received from the remote vehicle so that $t_0 = 0$ is the initial time. The left part of Fig. 3 visualizes this mechanism. At any t_k, if the state is in the opportunity region (i.e., $x(t_k) \in \mathcal{B}_P \cap \mathcal{A}_Q$), then the ego vehicle pursues the opportunity to merge ahead, but the decision will be reviewed at the next status update time t_{k+1}. If $x(t_k) \in \mathcal{A}_P$ (green region below the blue curve), the decision is set to merge ahead for $t \geq t_k$. Finally, if $x(t_k) \in \mathcal{C}_P \cap \mathcal{A}_Q$ (green region above the red boundary), then the decision is set to merge behind for $t \geq t_k$. We emphasize that in contrast to the conservative strategy (10) where the ego vehicle does not revise its decision, the decision checking (11) enables a potential decision change to merge ahead, which can improve the time efficiency of the ego vehicle.

B. Opportunistic Controller

The decision checking mechanism allows the ego vehicle to take the opportunity of merging ahead, but whether it can merge ahead or not also depends on the future motion of the remote vehicle, which we do not have control over. Here we propose a control algorithm that maximizes the ego vehicle's chance to merge ahead while ensuring that it can still merge behind without conflict if its decision to merge ahead is not possible. The key idea is to "push" the system toward the blue boundary, i.e., toward set $\mathcal{A}_P$, while keeping it inside the no-conflict set $\mathcal{A}_Q$. This can be formulated as an optimization problem as discussed below.

Let $T_{\text{reach},1}(t)$ denote the time needed for the remote vehicle to reach the conflict zone and $T_{\text{exit},2}(t)$ the time needed for ego vehicle to exit the conflict zone, calculated at time t assuming $[u_1(t), u_2(t)]^\top \equiv [a_{\max,1}, a_{\max,2}]^\top$ as future inputs. Based on the definition of sets $\mathcal{A}_P$ and $\mathcal{B}_P$, $x(t) \in \mathcal{A}_P$ if and only if $T_{\text{reach},1}(t) > T_{\text{exit},2}(t)$, while $T_{\text{reach},1}(t) \leq T_{\text{exit},2}(t)$ holds if $x(t) \in \mathcal{B}_P$. Define $\tilde{T}(t) := T_{\text{exit},2}(t) - T_{\text{reach},1}(t)$ and consider the state $x(t_k) \in \mathcal{B}_P \cap \mathcal{A}_Q$ such that $\tilde{T}(t_k) \geq 0$. In order for $x(t) \in \mathcal{A}_P$ at some $t > t_k$, $\tilde{T}(t) < 0$ must hold. Noting that $\tilde{T}(t)$ is a continuous function of t, pushing the state $x(t)$ from $\mathcal{B}_P$ to $\mathcal{A}_P$ is equivalent to decreasing $\tilde{T}(t)$ in t. Although we do not have control over $T_{\text{reach},1}(t)$, we can ensure via $u_2(t)$ that $T_{\text{exit},2}(t)$ decreases the most.

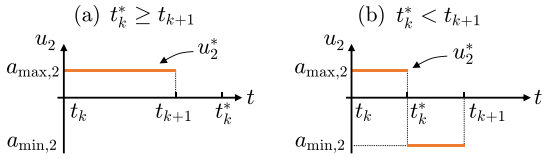

Fig. 4. Optimal solution $u_2^*(t)$ for the time interval $t \in [t_k, t_{k+1})$ (between receiving two adjacent status sharing packets) when $t_k^* \geq t_{k+1}$ (a) and when $t_k^* < t_{k+1}$ (b). Here t_k^* predicts the time when the state will reach the black boundary of set $\mathcal{A}_Q$.

Assuming $x(t_k) \in \mathcal{B}_P \cap \mathcal{A}_Q$, we formulate an optimization problem that minimizes the time derivative of $T_{\text{exit},2}(t)$ by shaping $u_2(t)$ within the time interval $[t_k, t_{k+1})$:

$$\begin{aligned} \min_{u_2(t) \in \mathbb{R}} \quad & J(t) = \frac{\mathrm{d}}{\mathrm{d}t} T_{\text{exit},2}(t), \quad \forall t \in [t_k, t_{k+1}), \\ \text{subject to} \quad & \text{dynamics (1)}, \\ & x(t_k) \in \mathcal{B}_P \cap \mathcal{A}_Q, \\ & x(t) \in \mathcal{A}_Q, \quad \forall t \in [t_k, t_{k+1}). \end{aligned} \tag{12}$$

Note that $\frac{\mathrm{d}}{\mathrm{d}t} T_{\text{exit},2}(t)$ depends on $u_2(t)$, and the optimal solution $u_2^*(t)$ ensures that $T_{\text{exit},2}(t)$ (and thus $\tilde{T}(t)$) decreases the most along $t \in [t_k, t_{k+1})$. This maximizes the opportunity of the state x evolving into the set $\mathcal{A}_P$. In the meantime, the last constraint ensures that a conflict-free merge behind is always possible.

Due to the simplicity of the dynamics (1), the optimal solution to (12) can be found analytically:

$$u_2^*(t) = \begin{cases} a_{\max,2}, & \text{if} \quad t \in [t_k, t_k^*), \\ a_{\min,2}, & \text{if} \quad t \in [t_k^*, t_{k+1}), \end{cases} \tag{13}$$

where t_k^* is the predicted time when the system state reaches the black boundary of set $\mathcal{A}_Q$ assuming $[u_1(t), u_2(t)]^\top \equiv [a_{\min,1}, a_{\max,2}]^\top$ for $t \geq t_k$. Since the future motion of vehicle 1 is unknown, we must assume the "worst-case scenario" $u_1(t) \equiv a_{\min,1}$ to ensure $x(t) \in \mathcal{A}_Q$. Note that $a_{\max,2}$ minimizes the cost function, while $a_{\min,2}$ ensures that the constraints are satisfied under the "worst case scenario" (see Appendix I for the proof). We remark that if $t_k^* \geq t_{k+1}$, then we only need to assign $u_2^*(t) \equiv a_{\max,2}$ for $t \in [t_k, t_{k+1})$, otherwise we switch to $a_{\min,2}$ at time t_k^*; see Fig. 4. Recursively, at t_{k+1} we check decision using $x(t_{k+1})$. If $x(t_{k+1}) \in \mathcal{B}_P \cap \mathcal{A}_Q$, then we calculate t_{k+1}^* and apply (13) again for $t \in [t_{k+1}, t_{k+2})$. One can prove that $t_{k+1}^* \geq t_k^*$, which means that status updates make the prediction less conservative.

Note that for $t_k^* < t_{k+1}$ (see Fig. 4(b)), if the remote vehicle's behavior does not follow the worst-case scenario, then $t_{k+1}^* > t_{k+1}$ holds. In this case, the optimal solution (13) switches from $a_{\max,2}$ to $a_{\min,2}$ at t_k^* and then back to $a_{\max,2}$ at t_{k+1}, which could result in passenger discomfort. Thus, for

practical purposes, one may implement a sub-optimal solution, where after the earliest t_k^* such that $t_k^* < t_{k+1}$ holds, the decision is changed to merge behind and $u_2(t) = a_{\min,2}$ is applied without pursuing the opportunity again. The value of $u_2(t)$ may be updated to be less conservative as new status updates are received, similar to the controller for merging behind proposed in [12].

As a summary, the control law (13) pursues the opportunity of merging ahead but ensures that a conflict-free merge behind is always possible. The decision checking mechanism (11) together with the corresponding controller is referred to as the opportunistic strategy. We remark that V2X communication is essential to apply this strategy as this allows the ego vehicle to monitor whether and when it crosses the blue boundary of $\mathcal{A}_P$. This will be demonstrated in the next section by simulations.

V. Simulation with Real Highway Data

In this section, we demonstrate the benefits of opportunistic strategy using simulations with real highway data, and compare the results with the conservative strategy. We show that the opportunistic strategy can significantly improve the time efficiency of the ego vehicle by revising decisions as new information becomes available via V2X.

To represent the remote vehicle, we use data collected from a real human-driven vehicle approaching a junction on highway US-23 near Ann Arbor, Michigan. The ego vehicle is assumed to be a connected automated vehicle merging from an on-ramp. At the initial time, the remote vehicle is 201.57 meters from the conflict zone traveling with speed 22.63 $[\mathrm{m/s}]$, while the ego vehicle is 210 meters from the conflict zone travelling with speed 25 $[\mathrm{m/s}]$. The magenta cross in Fig. 5(a) marks the initial state in the conflict chart, which is located in the opportunity region. In this case, the conservative strategy decides to merge behind, while the opportunistic strategy applies the decision checking mechanism (11) and controller (13) allowing the ego vehicle to eventually change its decision and merge ahead. Fig. 5(b)-(c) depict the system state as time evolves until the ego vehicle exits the conflict zone. The magenta crosses are plotted every 100 ms corresponding to 10 Hz status updates rate. Although both strategies avoid conflict, the opportunistic strategy significantly improves time efficiency of the ego vehicle by merging ahead within 29% shorter time. The corresponding time profiles are shown in Fig. 5(d)-(f) for the two different strategies. The conservative strategy updates the control input with status updates while keeping the decision the same. On the other hand, the opportunistic strategy is capable of updating the decision if such opportunity arises while still remaining conflict-free.

Figure 6(a)-(e) show the detailed evolution of trajectory under the opportunistic strategy. At 1.4 [s] (Fig. 6(b)), the trajectory crosses the blue boundary and enters set $\mathcal{A}_P$. Based on (11), the decision is changed to merge ahead, and the ego vehicle keeps using $a_{\max,2}$ to achieve this goal. However, if there is no status updates available when the state enters set $\mathcal{A}_P$, then a decision change is not possible.

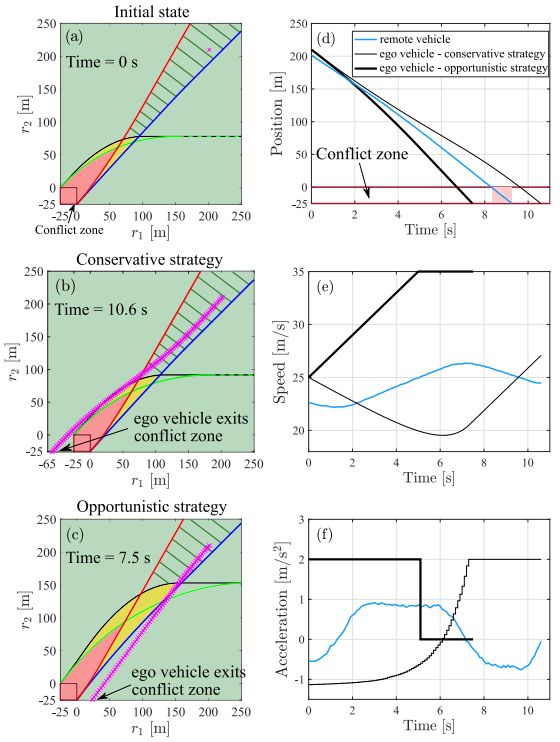

Fig. 5. Simulation results of conservative and opportunistic strategies with initial state $r_1(0) = 201.57$ [m], $v_1(0) = 22.63$ [m/s], $r_2(0) = 210$ [m], and $v_2(0) = 25$ [m/s] when status sharing packets are received every 0.1 [s]. (a) initial state in conflict chart (magenta cross). (b)-(c) trajectories under conservative and opportunistic strategies (magenta crosses); (d)-(f): position, speed and acceleration profiles.

Fig. 6(a)-(b), (f)-(i) show the evolution under opportunistic strategy without status update after the initial time. Although the trajectory crossed the blue boundary, the ego vehicle is not aware of it and, based on (13), the control input switches to $u_2(t) = a_{\min,2}$ at 3.1 [s] to keep the state inside $\mathcal{A}_Q$ (i.e., above the black boundary). At 4.3 [s], the state moves out of the $\mathcal{A}_P$ region, and the opportunity to merge ahead is gone. Eventually, the ego vehicle merges behind the remote vehicle using 16.3 [s] compared to 7.5 [s] in the regular status update case. These results are summarized in Table II. Consequently, maintaining regular V2X communication is essential to secure the benefits of opportunistic strategy.

VI. Conclusion

In this paper, we developed an opportunistic strategy for conflict prevention in cooperative maneuvering with the help of conflict analysis. We demonstrated that the proposed optimization-based strategy can significantly improve the time efficiency of the ego vehicle by revising its decision based on status updates received via V2X while guaranteeing a conflict-free maneuver. The benefits are illustrated by simulations using real highway data. We showed that V2X connectivity is essential to apply this strategy as regular status updates are needed for successful decision revision. Our future work include considering larger number of vehicles and moving conflict zones, and deriving communication requirements for securing the opportunity.

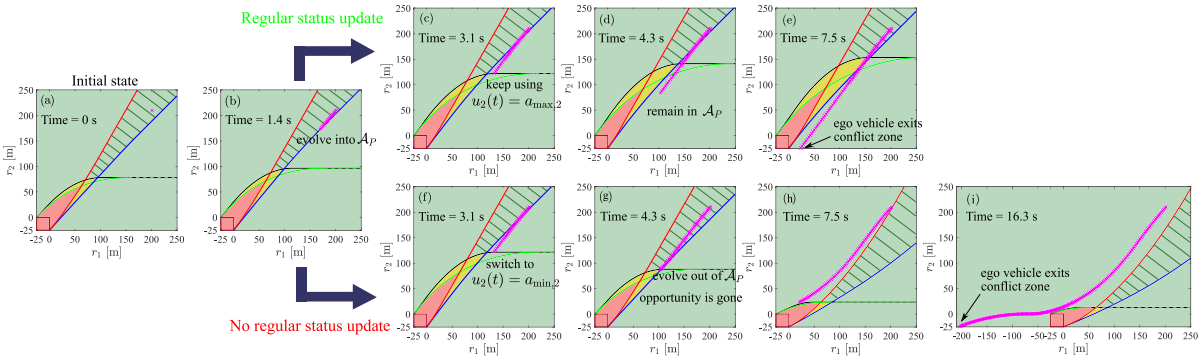

Fig. 6. Sequences of trajectories with and without regular status update. (a)-(e) ego vehicle changes decision to merge ahead based on status update at 1.4 [s] and keeps using $u_2(t) \equiv a_{\max,2}$ to merge ahead. (a)-(b), (f)-(i) opportunity to merge ahead is missed without status update. Here, the state evolves out of $\mathcal{A}_P$ at 4.3 [s] since the input $u_2(t) \equiv a_{\min,2}$ is used after 3.1 [s] to keep the state inside $\mathcal{A}_Q$ and the ego vehicle eventually merges behind.

TABLE II

SIMULATION RESULTS WITH EGO VEHICLE'S INITIAL STATE $r_2(0) = 210$ [m] AND $v_2(0) = 25$ [m/s].

V2X condition	Regular status update		No regular status update	
Strategy	Conservative	Opportunistic	Conservative	Opportunistic
Maneuver result	merge behind	merge ahead	merge behind	merge behind

APPENDIX I
PROOF OF THE OPTIMALITY OF SOLUTION (13)

From the dynamics (1), one can calculate

$$T_{\text{exit},2}(t) = \tag{14}$$
$$\begin{cases} \frac{\sqrt{v_2^2(t)+2a_{\max,2}(r_2(t)+s)}-v_2(t)}{a_{\max,2}}, & \text{if } r_2(t) \le \frac{v_{\max,2}^2-v_2^2(t)}{2a_{\max,2}} - s, \\ \frac{v_{\max,2}-v_2(t)}{a_{\max,2}} + \frac{r_2(t)+s}{v_{\max,2}} - \frac{v_{\max,2}^2-v_2^2(t)}{2a_{\max,2}v_{\max,2}}, & \text{otherwise.} \end{cases}$$

which yields that

$$J(t) = \frac{\mathrm{d}}{\mathrm{d}t} T_{\text{exit},2}(t) = \tag{15}$$
$$\begin{cases} -f_1(t)\,\mathrm{sat}\big(u_2(t)\big) - f_2(t), & \text{if } r_2(t) \le \frac{v_{\max,2}^2-v_2^2(t)}{2a_{\max,2}} - s, \\ -g_1(t)\,\mathrm{sat}\big(u_2(t)\big) - g_2(t), & \text{otherwise,} \end{cases}$$

where

$$\begin{aligned} f_1(t) &= \frac{1}{a_{\max,2}}\left(1 - \frac{v_2(t)}{\sqrt{v_2^2(t)+2a_{\max,2}(r_2(t)+s)}}\right), \\ f_2(t) &= \frac{v_2(t)}{\sqrt{v_2^2(t)+2a_{\max,2}(r_2(t)+s)}}, \qquad (16) \\ g_1(t) &= \frac{1}{a_{\max,2}}\left(1 - \frac{v_2(t)}{v_{\max,2}}\right), \qquad g_2(t) = \frac{v_2(t)}{v_{\max,2}}. \end{aligned}$$

Thus, from (15), for all $t \in [t_k, t_{k+1})$, independent of the value of $r_2(t)$ and $v_2(t)$, maximizing $\mathrm{sat}\big(u_2(t)\big)$ minimizes the cost function $J(t)$. This implies $u_2(t) \equiv a_{\max,2}$. Moreover, the constraint $x(t) \in \mathcal{A}_Q$ must hold. Since vehicle 1's status is unknown until t_{k+1}, we must assume the worst-case scenario $u_1(t) \equiv a_{\min,1}$ for $t > t_k$, and predict time t_k^* such that $x(t_k^*)$ reaches the boundary of $\mathcal{A}_Q$. Based on the definition of $\mathcal{A}_Q$, $a_{\min,2}$ is the only input that can keep a state staying on the boundary of $\mathcal{A}_Q$ under the worst-case scenario. Therefore, (13) is the optimal solution to (12).

REFERENCES

[1] L. Hobert, A. Festag, I. Llatser, L. Altomare, F. Visintainer, and A. Kovacs, "Enhancements of V2X communication in support of cooperative autonomous driving," *IEEE Communications Magazine*, vol. 53, no. 12, pp. 64–70, 2015.

[2] B. Lehmann, H. J. Günther, and L. Wolf, "A generic approach towards maneuver coordination for automated vehicles," in *21st IEEE International Conference on Intelligent Transportation Systems (ITSC)*, 2018, pp. 3333–3339.

[3] I. Llatser, T. Michalke, M. Dolgov, F. Wildschütte, and H. Fuchs, "Cooperative automated driving use cases for 5G V2X communication," in *2nd IEEE 5G World Forum (5GWF)*, 2019, pp. 120–125.

[4] J. Rios-Torres and A. A. Malikopoulos, "A survey on the coordination of connected and automated vehicles at intersections and merging at highway on-ramps," *IEEE Transactions on Intelligent Transportation Systems*, vol. 18, no. 5, pp. 1066–1077, 2016.

[5] A. I. M. Medina, N. van de Wouw, and H. Nijmeijer, "Automation of a T-intersection using virtual platoons of cooperative autonomous vehicles," in *the 18th International Conference on Intelligent Transportation Systems*, Las Palmas, Spain, 2015, pp. 1696–1701.

[6] R. Kianfar, P. Falcone, and J. Fredriksson, "Safety verification of automated driving systems," *IEEE Intelligent Transportation Systems Magazine*, vol. 5, no. 4, pp. 73–86, 2013.

[7] SAE J3216, "Taxonomy and Definitions for Terms Related to Cooperative Driving Automation for On-Road Motor Vehicles," SAE International, Tech. Rep., 2020.

[8] J. I. Ge, S. S. Avedisov, C. R. He, W. B. Qin, M. Sadeghpour, and G. Orosz, "Experimental validation of connected automated vehicle design among human-driven vehicles," *Transportation Research Part C*, vol. 91, pp. 335–352, 2018.

[9] S. S. Avedisov, G. Bansal, and G. Orosz, "Impacts of connected automated vehicles on freeway traffic patterns at different penetration levels," *IEEE Transactions on Intelligent Transportation Systems*, 2021. [Online]. Available: https://doi.org/10.1109/TITS.2020.3043323

[10] M. R. Hafner and D. Del Vecchio, "Computational tools for the safety control of a class of piecewise continuous systems with imperfect information on a partial order," *SIAM Journal on Control and Optimization*, vol. 49, no. 6, pp. 2463–2493, 2011.

[11] M. R. Hafner, D. Cunningham, L. Caminiti, and D. Del Vecchio, "Cooperative collision avoidance at intersections: Algorithms and experiments," *IEEE Transactions on Intelligent Transportation Systems*, vol. 14, no. 3, pp. 1162–1175, 2013.

[12] H. M. Wang, T. G. Molnár, S. S. Avedisov, A. H. Sakr, O. Altintas, and G. Orosz, "Conflict analysis for cooperative merging using V2X communication," in *31st IEEE Intelligent Vehicles Symposium*, Las Vegas, USA, 2020, pp. 1538–1543.

[13] SAE J2735, "Dedicated Short Range Communications (DSRC) Message Set Dictionary Set," SAE International, Tech. Rep., 2016.